PHYSICAL REVIEW B **87**, 060103(R) (2013)

Stand-off dislocations at a twist grain boundary in gold as seen via high-resolution transmission electron microscopy

Sung Bo Lee,[1,*] Yanghoo Kim,[1] Young-Min Kim,[2] Seung Jo Yoo,[2] Heung Nam Han,[1,†] and Dong Nyung Lee[1]

[1]*Department of Materials Science and Engineering and Center for Iron & Steel Research, RIAM, Seoul National University, Seoul 151-744, Republic of Korea*

[2]*Korea Basic Science Institute, Daejeon 305-806, Republic of Korea*

(Received 25 October 2012; revised manuscript received 19 December 2012; published 19 February 2013)

The present study applies high-resolution transmission electron microscopy with a combination of geometric phase analysis to characterize atomic structures of a twist grain boundary in gold, illuminating the presence of misfit dislocations with a stand-off distance from the grain boundary. The formation of the stand-off misfit dislocations is attributed to a difference in shear modulus between the two grains bordering the grain boundary, which originates in elastic anisotropy of Au.

DOI: 10.1103/PhysRevB.87.060103 PACS number(s): 61.72.Ff, 61.72.Mm, 62.20.de, 68.37.Og

The misfit at an interface between two crystalline phases is accommodated by misfit dislocations, which are located directly at the interface.[1] However, if the shear moduli are different for two phases, misfit dislocations are repelled to the region with the lower modulus. That is, the misfit dislocations exhibit a stand-off distance from the interface, because the dislocation energy is lower in the more compliant region.[2–5] The stand-off distance is accepted as being determined by the balance between image forces due to the difference in elastic constants between two crystals adjoining at the interface and coherency forces due to the lattice mismatch of the crystals calculated by using linear elastic approximation.[2–5] Their calculations indicate that the equilibrium stand-off distance increases with increasing ratio of the shear moduli and with decreasing misfit. The theoretical treatments of the formation of stand-off dislocations have been applied to experimental observation of heterophase interfaces, e.g., metal-oxide ceramic systems.[6–10] However, if a material is elastically anisotropic, two grains bordering a grain boundary (GB) may produce a difference in shear modulus, under which misfit dislocations will be repelled from the GB and moved into the more compliant one.

Here, we report observations of stand-off dislocations at a homophase interface (here, a twist GB with a misorientation of 45°/[010] in Au) by high-resolution transmission electron microscopy (HRTEM). The bicrystalline TEM specimen was composed of two grains with surface normal directions of [001] and [−101]. Interestingly, misfit dislocations did not lie exactly at the GB, but their cores were positioned a few atomic layers away from the GB into the (001) grain. The observation is successfully clarified by elastic anisotropy of Au, whose Zener's anisotropy factor $[2(S_{11} - S_{12})/S_{44}]$ is ∼2.9, where S_{ij}'s are the elastic compliances. When the factor is unity, the elastic properties are isotropic. It follows that Au is a highly anisotropic material. Our calculations of shear modulus based on elastic anisotropy of Au reveal that the (001) grain is more compliant than the (−101) grain, which is in agreement with the observation. The shear modulus difference varies with the GB plane normal (GB inclination), a dependence that has not been elucidated so far. GBs are very important for materials performance in many technical applications.[11] For understanding physical phenomena associated with GBs, knowledge of the GB-related defect structure is crucial. Our study promotes an understanding of the GB-related defect structure.

In this study, we used a 99.999% pure Au bicrystal having a *twist* GB with a misorientation of 45°/[010]. The bicrystal was fabricated by diffusion bonding (MaTeck). TEM specimens were prepared from the bicrystal on a focused Ga-ion beam (FIB) workstation. Cross-section FIB lamellae were Pt-welded to a Mo half-grid for TEM. The prepared specimens were heated up (at a rate of 15 °C/min) and annealed at 600 °C for 2 h without the electron beam in a high-voltage TEM operating at 1.25 MeV (JEM-ARM1300S, JEOL). After cooling to room temperature they were observed in the same microscope. The *ex situ* observation was employed to exclude knock-on damage by the 1.25 MeV electron beam, which amounts to the threshold value for Frenkel pair formation for Au (∼1.2 MeV). The thickness of the specimens was determined by an electron-energy-loss-spectroscopy log-ratio method[12] to be 33–50 nm. Quantitative measurements of local strain components near the GB were made by geometric phase analysis (GPA),[13,14] a TEM strain mapping technique, with a spatial resolution of 0.41 nm. The strain artifact in the phase images arising from the electron optical lens distortion introduced by the microscope was calibrated for the accuracy of the strain measurements to be better than 0.1%.

As shown in Fig. 1(a), the GB was observed to be smoothly curved before annealing. After annealing, the GB was observed to be faceted with flat $(010)_A//(010)_B$ $[(010)_{A,B}]$ terraces separated by occasional atomic-scale height steps [Fig. 1(b)], where the grain with the surface normal orientation of [001] is designated as A and the other grain as B. The average separation distance was ∼6 nm. And interestingly, an array of dislocations appeared in grain A, being aligned along the GB, as shown in Fig. 1(c). Their cores were positioned away from the GB, a stand-off distance being two times the interplanar spacing of the $(020)_{Au}$ planes. A Burgers circuit made around the core region produces a closure failure [Fig. 1(c)]. Since HRTEM projects a two-dimensional image of a material, the observed closure failure of the Burgers circuit was a projection of a real Burgers vector, in this case, onto the (001) plane. The projected Burgers vector was $a/2[100]$, with a being the lattice parameter of Au. The Burgers vector corresponds to

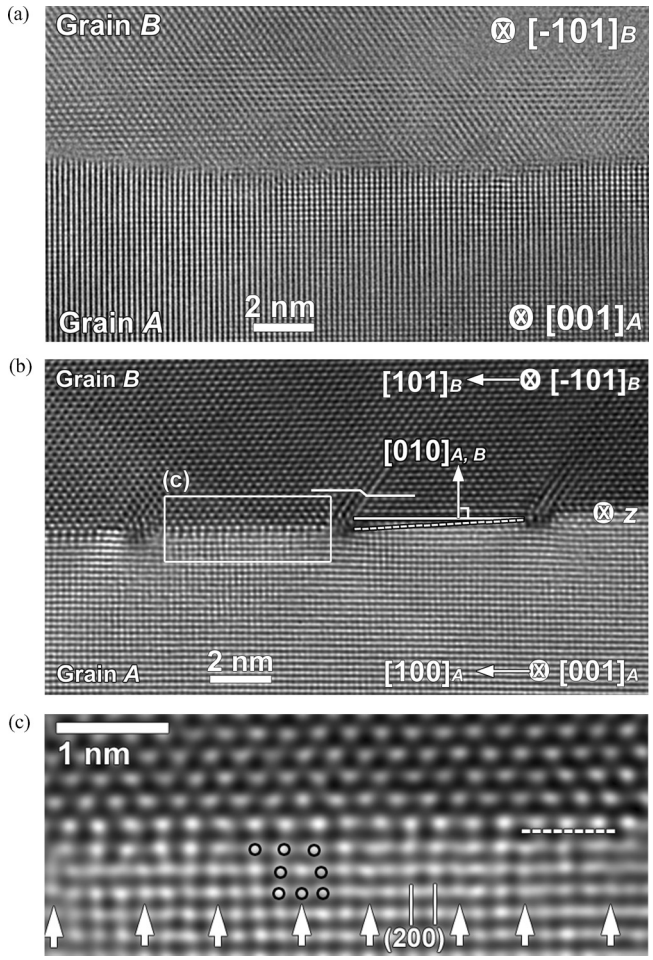

FIG. 1. HRTEM images of a twist GB with a misorientation of 45°/[010] (a) before and (b) after annealing. (c) Enlarged view of a boxed region in (b). A dashed line in (b) indicates the average GB inclination angle of ∼2.85° from the $(010)_A$//$(010)_B$ plane about the z direction. Stacking faults are seen in grain B, as marked by a white-kinked line in the middle of (b). Stand-off dislocations formed in grain A can be seen in (c). The GB position is indicated by a dashed line.

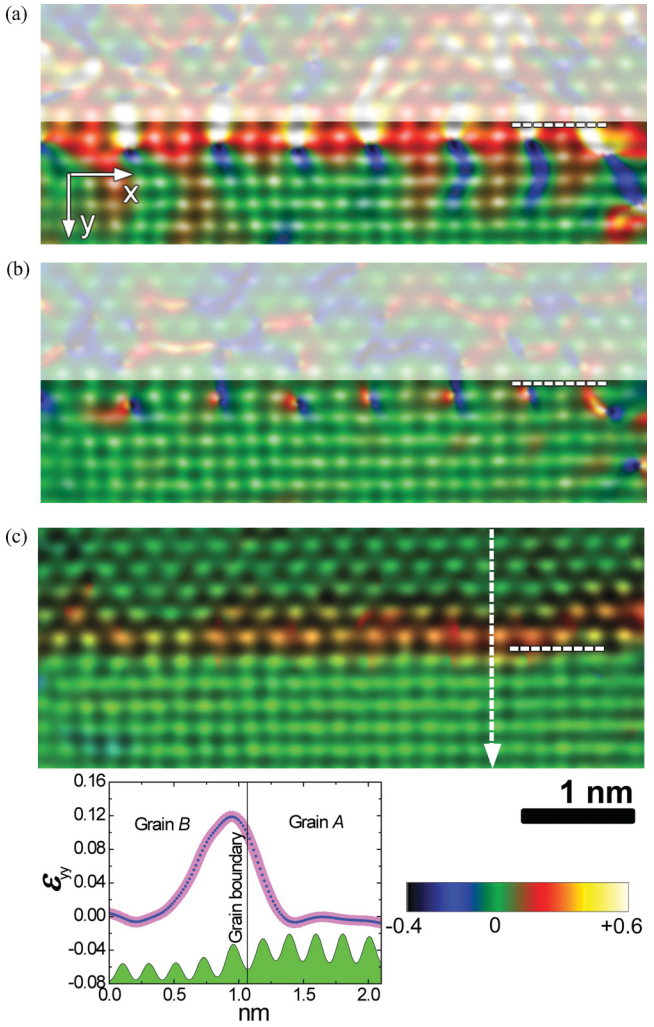

FIG. 2. (Color) Strain fields of (a) $\boldsymbol{\varepsilon}_{xx}$, (b) $\boldsymbol{\varepsilon}_{xy}$, and (c) $\boldsymbol{\varepsilon}_{yy}$ around the stand-off dislocations obtained by GPA. The x and y directions are chosen to be parallel and normal to the GB, respectively. All the strain maps are superimposed on the HRTEM image shown in Fig. 1(c). The strain field of $\boldsymbol{\varepsilon}_{yy}$ is also measured across the GB (indicated by a dashed arrow) as a line graph in (c). The GB position is indicated by a dashed line. The color bar indicates the full strain range from -0.4 to 0.6.

$a/2\langle 101\rangle$, because it is the shortest vector allowed in Au and thus has the lowest dislocation energy. The Burgers vector was parallel to the GB plane [i.e., $(010)_{A,B}$ in Fig. 1(b)] at an angle of 45° with the $[100]_A$ direction. The atomic columns at the cores appear to be missing, suggesting that the dislocation line ran parallel to the $[001]_A$ direction, which is the specimen thickness direction. This might result from a reduction of dislocation line energy. The spacings between the stand-off dislocations show a repeat of two kinds of periods, three and four times the interplanar spacing of the (200) planes ($a/2$, where a is the lattice parameter of Au).

As a result, the Burgers vector and dislocation line formed an angle of 45° and the slip plane, determined by the Burgers vector and dislocation line, is taken to be parallel to the $(010)_A$, which is not the slip plane in face-centered-cubic materials. The observations indicate that the dislocations were sessile and mixed. What was observed is the edge component of the dislocations.

As shown in Fig. 2, strain fields $\boldsymbol{\varepsilon}_{xx}$, $\boldsymbol{\varepsilon}_{xy}$, and $\boldsymbol{\varepsilon}_{yy}$ around the stand-off dislocations were analyzed by GPA at the subnanometer scale. ε_{xx} exactly indicates the position of cores of the stand-off dislocations [Fig. 2(a)]. For positive edge dislocations, the structure above the slip plane is compressed owing to the presence of the extra-half plane and that below is expanded. Figure 2(a) shows that strong tensile strain fields appear close to the GB and compressive strain fields are distant from the GB, as indicated by the color bar (−40 to +60%), which indicates an approximate position of the extra-half plane. In the map of $\boldsymbol{\varepsilon}_{xy}$ in Fig. 2(b) the shear strain changes the sign from left to right with the core as the center, which is characteristic of edge-type dislocations. [The GPA maps shown in Figs. 2(a) and 2(b) were referred to as grain A. Thus the region above a dashed line indicating the GB position (grain B) is not relevant, since it has no phase relation with grain A, showing featureless noise. Opaque rectangles are thus superimposed on grain B.] Figure 2(c) shows the map of $\boldsymbol{\varepsilon}_{yy}$, which applies to both the grains because the y direction

is [010] and is common to both grains. Interestingly, strong tensile strain fields developed in the region of grain B grain bordering the GB.

Since normal and shear stress components acting on the free surface of a body are zero, the stress state of a thin film can approximate to plane stress, which holds for the bicrystalline TEM specimen in this study. Therefore, $\sigma_{zz} = \sigma_{zx} = \sigma_{zy} \approx 0$, where the z direction is normal to the specimen surface and parallel to the $[001]_A$ (or $[-101]_B$) direction [Fig. 1(b)]. The *effective misfit-stress component* would act along the GB plane, and under the plane stress state, is approximated to be parallel to the GB *length* direction, which is parallel to the GB plane without any z-direction component, because there is no stress component parallel to the z direction under this condition. Therefore, we can simply consider the misfit along one direction, i.e., the GB length direction. The lattice planes normal to the x direction have different spacings for the two grains (d_A for grain A and d_B for grain B). The spacing d_A corresponds to interplanar spacing of the (200) planes of Au ($a/2$) and d_B to the interplanar spacing of the (101) planes ($a/\sqrt{2}$). The periodic spacing **D** between adjacent parallel stand-off dislocations in grain A is obtained by calculating the vernier period of the misfit **P** in the GB length direction:

$$\mathbf{D} = \mathbf{P}d_B = (P+1)d_A, \qquad \text{because } d_B \text{ is larger than } d_A.$$

P is calculated to be 2.451. Thus the spacing between the stand-off dislocations in grain A is calculated to have a period of 3.451, which agrees with the observed value of 3.5 [the mean quantity of the two repeat periods (3,4)] as shown in Fig. 1(c).

The GPA analyses (Fig. 2) demonstrate the formation of stand-off dislocations in grain A. The atomic layers in grain B undergoing strong tensile normal strain in the y direction [Fig. 2(c)] are attributed to the strong tensile strain near the core of the stand-off dislocations in the x direction [Fig. 2(a)]. The tensile strain is expected to cause tensile strain to the coherently strained region in grain B in the y direction by Poisson's effect.

The previous studies based on linear elasticity theory[2–5] suggest that any difference in shear modulus between joined regions would repel misfit dislocations from the interface. For materials of cubic symmetry, the shear modulus G for a certain plane and direction is given by a function of elastic compliances and direction cosines, a_{ij}:[15]

$$1/(4G) = (1/4)\,S_{44} + [S_{44} - 2\,(S_{11} - S_{12})] \times (a_{11}a_{21}a_{12}a_{22} + a_{11}a_{21}a_{13}a_{23} + a_{12}a_{22}a_{13}a_{23}),$$

where the direction cosines a_{ij} relate the arbitrary directions x_i' to the fundamental axes of the material x_j. The fundamental axes of a cubic material x_1, x_2, and x_3, are three axes of fourfold symmetry, i.e., [100], [010], and [001]. x_1' corresponds to the shear direction $[HKL]$ and x_2' to the shear plane normal direction, whereupon we designate the shear modulus as $G_{(hkl)[HKL]}$. For Au, $S_{11} = 0.0310$, $S_{12} = -0.0144$, and $S_{44} = 0.0294$ GPa^{-1} at 600 °C (the annealing temperature),[16,17] which were used for the calculation of the shear moduli.

To calculate the shear modulus difference in our case, first of all, relevant shear planes and directions for the two grains should be selected. In the present study, the shear plane is set parallel to the GB plane. Under the plane stress state, the shear direction is set parallel to the GB length direction, as for the effective misfit stress. The GB before annealing was smoothly curved [Fig. 1(a)]. We suggest that the defaceted morphology before annealing is related to the occurrence of the stand-off dislocation. As will be shown later, if the GB is parallel to the $(010)_{A,B}$, no shear modulus difference is calculated between the two grains. The inclination from the $(010)_{A,B}$ plane produces a shear modulus difference. From the faceted structure observed after annealing [Fig. 1(b)], the average inclination angle is measured to be ~2.85° from the $(010)_{A,B}$ about the z direction, as indicated by the dashed line shown in Fig. 1(b). For the present, we set both the shear planes and directions for the two grains parallel to the inclined GB plane with an inclination of 2.85°.

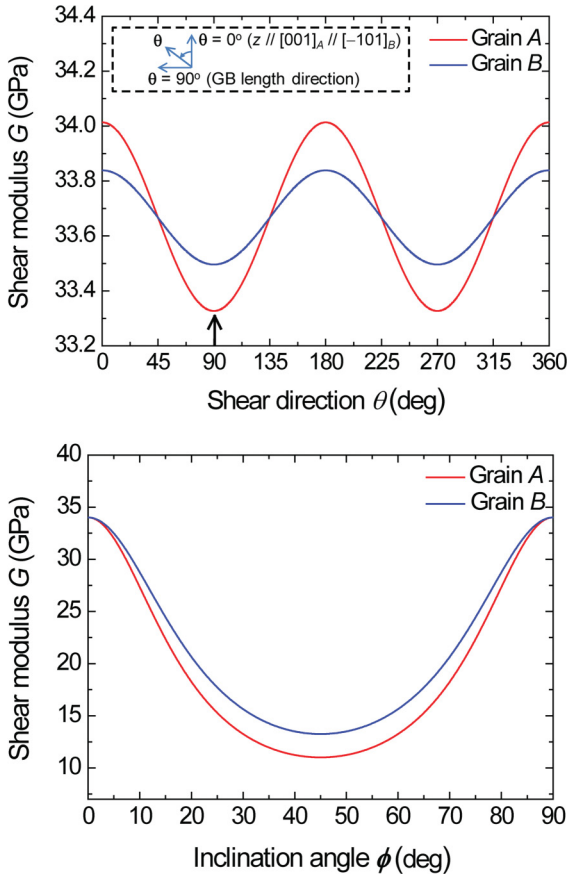

FIG. 3. (Color) (a) Plots of shear moduli in directions on the shear planes of grains A and B which are parallel to the inclined GB plane with an inclination angle of 2.85°. A dashed rectangle (inset) represents the shear planes parallel to the inclined GB plane. In (b), shear moduli for grains A and B are plotted in the shear direction on the shear plane whose normal is rotated by ϕ from the $[010]_{A,B}$ about the z direction [indicated in Fig. 1(b)].

If the shear moduli are plotted on the shear planes set parallel to the 2.85°-inclined GB as a function of direction including the GB length direction, we obtain Fig. 3(a), where the abscissa refers to the angle between a shear direction and the z direction. The GB length direction corresponds to $\theta = 90°$. For $\theta = 90°$, the shear modulus for grain A is calculated to be 33.33 GPa and that for grain B is 33.50 GPa at

600 °C. Thus grain A is more compliant than grain B under the *plane stress state*, misfit dislocations being repelled to grain A, which is in agreement with the present observation.

Because of the wavy morphology of the GB before annealing [Fig. 1(a)], actual inclination angles varied from point to point along the GB. Thus it would become a more general case if the shear moduli for grains A and B are plotted on the shear plane whose normal is rotated from the $[010]_{A,B}$ about the z direction [Figs. 1(b) and 3(b)]. The shear moduli at the inclination angle ϕ of 2.85° correspond to the modulus values mentioned above. The plot demonstrates that, once the GB plane deviates from $(010)_{A,B}$, a shear modulus difference is induced and grain A is more compliant.

If the GB plane is exactly parallel to $(010)_{A,B}$, corresponding to $\phi = 0°$, no shear modulus difference is expected, and thus stand-off dislocations are not likely to occur. It is therefore deduced that the dislocations formed *before* the GB faceting. And even after the GB was faceted with the $(010)_{A,B}$ terraces, since the dislocations were sessile, they would not be annihilated.

The thermal strain might influence the GB structure in our case. The linear thermal expansion coefficients α of Au, Mo (TEM grid), and Pt (for welding) are 14.2×10^{-6}, 5×10^{-6}, and 9×10^{-6} K^{-1}, respectively. The thermal strain ($\Delta\alpha\Delta T$) upon heating and cooling between the annealing temperature of 600 °C and room temperature approximates to an order of 10^{-3}. This is negligible, compared with the lattice misfit strain $[2(d_B - d_A)/(d_B + d_A)$, where d_A and d_B are interplanar spacings of the (200) and (101) planes, respectively, as specified above] of 0.343, leading us to conclude that the thermal strain is unlikely to affect the GB structure. The emission of partial dislocations into grain B [(Fig. 1(b)] is concluded to be induced by the misfit stress.

Merkle *et al.*[18,19] examined atomic structures of a twist GB with the same misorientation as ours. However, their observation does not give any indication for misfit localization and stand-off dislocations at the GB. The GB was just flat, parallel to the (010) plane, and aperiodic. We attribute the nonobservation of stand-off dislocations to their thin TEM specimen thicknesses (5–10 nm;[18] 33–50 nm for our case). As a TEM specimen becomes thinner, the strain energy arising from the misfit at a GB in the specimen decreases. Below a critical specimen thickness, where the strain energy is inadequate to compensate for the dislocation energy, (stand-off) misfit dislocations are unlikely to form, as suggested by Refs. 1 and 20.

To conclude, the present investigation indicates that the presence of misfit stand-off dislocations is not limited to heterophase interfaces. Our study demonstrates direct evidence of stand-off dislocations at a homophase interface (here, a twist GB in Au). Their formation at the Au GB is attributed to the difference in shear modulus between two grains bordering the GB, which is caused by elastic anisotropy in Au. This study illuminates that the shear modulus difference strongly depends on GB inclination.

This research was supported by the Basic Science Research Program (2011-0027382) through the National Research Foundation of Korea, funded by the Ministry of Education, Science and Technology. H.N.H. and D.N.L. acknowledge Grant No. 0417-20110114 from RIAM in Seoul National University.

*bolee@snu.ac.kr

†hnhan@snu.ac.kr

[1] F. C. Frank and J. H. van der Merwe, Proc. R. Soc. London, Ser. A **198**, 216 (1949).

[2] M. Yu. Gutkin, M. Militzer, A. E. Romanov, and V. I. Vladimirov, Phys. Status Solidi A **113**, 337 (1989).

[3] M. Yu. Gutkin and A. E. Romanov, Phys. Status Solidi A **127**, 117 (1992).

[4] S. V. Kamat, J. P. Hirth, and B. Carnahan, Mater. Res. Soc. Symp. Proc. **103**, 55 (1988).

[5] W. Mader and D. Knauss, Acta Metall. Mater. (Suppl.) **40**, S207 (1992).

[6] W. Mader, Mater. Res. Soc. Symp. Proc. **82**, 403 (1987).

[7] M. Kuwabara, J. C. H. Spence, and M. Rühle, J. Mater. Res. **4**, 972 (1989).

[8] F.-S. Shieu and S. L. Sass, Acta Metall. **38**, 1653 (1990).

[9] K. L. Merkle, M. I. Buckett, and Y. Gao, Acta Metall. Mater. (Suppl.) **40**, S249 (1992).

[10] P. Lu and F. Cosandey, Ultramicroscopy **40**, 271 (1992).

[11] A. Sutton and R. W. Balluffi, *Interfaces in Crystalline Materials* (Clarendon Press, Oxford, 1995).

[12] T. Malis, S. C. Cheng, and R. F. Egerton, J. Electron Microsc. Tech. **8**, 193 (1988).

[13] M. J. Hÿtch, E. Snoeck, and R. Kilaas, Ultramicroscopy **74**, 131 (1998).

[14] E. Snoek, B. Warot, H. Ardhuin, A. Rocher, M. J. Casanove, R. Kilaas, and M. J. Hÿtch, Thin Solid Films **319**, 157 (1998).

[15] C. N. Reid, *Deformation Geometry for Materials Scientists* (Pergamon, Oxford, 1973).

[16] S. M. Collard and R. B. McLellan, Acta Metall. Mater. **39**, 3143 (1991).

[17] S. M. Collard, Ph.D. dissertation, Rice University, 1991.

[18] K. L. Merkle and L. J. Thompson, Mater. Lett. **48**, 188 (2001).

[19] K. L. Merkle and L. J. Thompson, Phys. Rev. Lett. **83**, 556 (1999).

[20] J. R. Willis, S. C. Jain, and R. Bullough, Philos. Mag. A **62**, 115 (1990).